The International Journal of Cardiovascular Imaging (2019) 35:917–926
https://doi.org/10.1007/s10554-018-1513-z

ORIGINAL PAPER

Comparison of the different imaging time points in delayed phase cardiac CT for myocardial scar assessment and extracellular volume fraction estimation in patients with old myocardial infarction

Ahmed Hamdy[1] · Kakuya Kitagawa[1] · Yoshitaka Goto[1] · Akimasa Yamada[1] · Satoshi Nakamura[1] · Masafumi Takafuji[1] · Naoki Nagasawa[1] · Hajime Sakuma[1]

Received: 23 August 2018 / Accepted: 11 December 2018 / Published online: 18 December 2018

Abstract

Delayed enhancement cardiac CT is a potential tool for myocardial viability assessment and is essential for extracellular volume fraction (ECV) estimation with CT. The objective of this study is to determine the optimal delay time for acquisition of delayed CT scans. Thirty-five patients with enhancement pattern typical of previous myocardial infarction on delayed CT and 17 control subjects comprised the study population. Delayed scans were acquired at 3, 5 and 7 min after contrast material injection. Image quality and estimated ECV were compared among the three time points. Delayed CT at 5 min showed the highest signal-to-noise ratio of 15.2 ± 1.0 [$p < 0.0001$; vs. 3 min (13.6 ± 1.0), $p = 0.0015$; vs. 7 min (14.9 ± 1.0)]. Contrast-to-noise ratio of infarcted and remote myocardium was highest at 7 min (6.4 ± 2.5), but was not significantly different from 5 min (6.1 ± 2.2, $p = 0.08$). The ECV values were constant over the three time points, although, in segments containing infarcted myocardium, trend of lower values was noted at 3 min compared to 5 and 7 min. ECV values at 5 min was 27.1% ± 2.1% in control subjects, 27.2% ± 3.0% in remote segments of patients with infarction, and 39.6% ± 5.3% in segments containing infarcted myocardium. Myocardial scars are equally best visualized with delay time of 5 and 7 min post contrast administration. No significant difference was observed in ECV of healthy myocardium or focal scars among delay time of 3, 5, and 7 min. Delay time of 5 min after contrast injection may be recommended for CT delayed enhancement imaging.

Keywords Diagnostic cardiac imaging · Cardiovascular disease · Myocardial infarction · Myocardial viability assessment · Extracellular volume fraction · X-ray computed tomography

Introduction

Cardiac computed tomography (CT) delayed enhancement has emerged as a potential tool for the assessment of myocardial viability in the last decade with remarkable advances in image acquisition, reconstruction, and post-processing [1–3]. Delayed enhancement CT is an important approach by which cardiac CT can detect regional fibrosis associated with ischemic injury and cardiomyopathies. Moreover, recent studies suggested potential usefulness of CT delayed enhancement as a modality to estimate extracellular volume (ECV) fraction, which reflects the amount of myocardial fibrosis. Delayed enhancement and ECV determined by CT may have prognostic and therapeutic implications, as we have learned from extensive magnetic resonance imaging literature [4–7]. However, no consensus has been available on which time point after contrast injection should be used for delayed CT acquisition in order to achieve accurate assessment of myocardial scars and ECV estimation. This is of particular importance, as the short delay time may result in insufficient contrast material accumulation for visualization of infarct scar, while long delay time may suffer from low contrast-to-noise due to excessive contrast wash out [8, 9]. Human studies reported a wide range of time points for

This paper was presented as an oral abstract at the European society of cardiovascular radiology (ESCR), 2018 and was awarded the certificate of merit from the scientific committee.

Electronic supplementary material The online version of this article (https://doi.org/10.1007/s10554-018-1513-z) contains supplementary material, which is available to authorized users.

✉ Kakuya Kitagawa
kakuya@clin.medic.mie-u.ac.jp

[1] Mie University Hospital, 2-174 Edobashi, Tsu, Mie 514-8507, Japan

delayed image acquisition ranging from 5 up to 15 min after contrast administration [3, 10–18]. The purpose of this study was to determine the single delayed imaging time point with the highest image quality for infarct scar visualization and to study the effect of different imaging time points on the ECV estimation.

Materials and methods

Study population

This study was approved by the institutional review board and written informed consent for participation in the study was obtained from all patients.

Comprehensive cardiac CT study described in the next section was performed in 139 patients with known or suspected coronary artery disease between December 2015 and November 2016 in our institution. Among them, we recruited 35 patients (31 men and 4 women; age 67.5 ± 11 years) showing delayed enhancement typical of previous myocardial infarction (MI) (i.e. involving the sub-endocardium and confined to the vascular territory of a coronary artery) on delayed phase CT in this study for image quality assessment and ECV estimation (Fig. 1). The mean age of the myocardial infarct in these patients was 8.9 ± 7 years.

Of the remaining 104 subjects without ischemic pattern of delayed enhancement, 17 subjects (14 males and 3 females, age 64.5 ± 10.3 years) were also enrolled in this study as control subjects for ECV estimation. In the selection of the control subjects, subjects with history of or current obstructive coronary artery disease on coronary CT angiography (n = 61), myocardial delayed enhancement other than MI (n = 5), cardiac-involving systemic diseases and predisposing factors for coronary artery disease (hypertension, diabetes, dyslipidemia and smoking, n = 21) were excluded.

Baseline characteristics of the study population are presented in Table 1.

CT data acquisition and reconstruction

All cardiac CT examinations were performed using a third generation dual-source CT system (Somatom Force; Siemens Healthcare, Forchheim, Germany). Our comprehensive cardiac CT study consisted of unenhanced CT, stress dynamic perfusion CT, coronary CT angiography, and delayed-phase CT. After obtaining the scout images of the entire chest, unenhanced CT for the subsequent ECV estimation was performed with the same acquisition protocol used for delayed-phase CT as will be discussed. Stress dynamic myocardial perfusion CT was performed with a bolus injection of 40 mL of iodinated contrast agent with an iodine concentration of 370 mgI/mL (Iopamiron

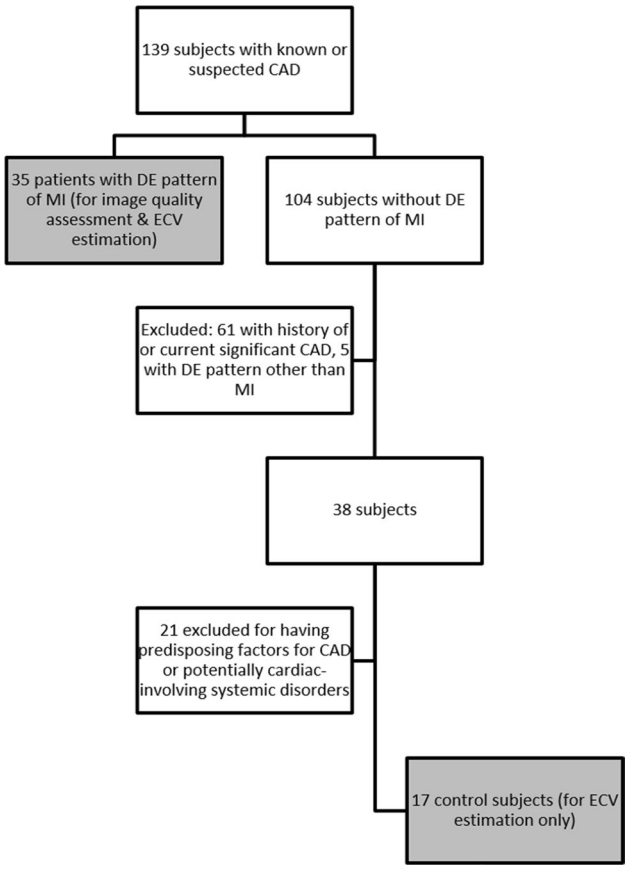

Fig. 1 Selection chart of patients and control subjects

Table 1 Baseline characteristics of the study population

	Patients	Controls
Mean age (years)	67.5 ± 11	64.5 ± 10
Male sex [n (%)]	31 (89)	14 (82)
Body mass index		
Normal < 25 kg/m^2 [n (%)]	20 (57)	16 (94)
Overweight 25–30 kg/m^2 [n (%)]	12 (34)	1 (6)
Obese 30–40 kg/m^2 [n (%)]	3 (9)	0 (0)
Risk factors		
Hypertension [n (%)]	26 (74)	0 (0)
Dyslipidemia [n (%)]	27 (77)	0 (0)
Diabetes [n (%)]	15 (43)	0 (0)
Smoking [n (%)]	26 (74)	0 (0)
Prior PCI [n (%)]	27 (77)	0 (0)
Prior CABG [n (%)]	8 (23)	0 (0)
History of myocardial infarction [n (%)]	27 (77)	0 (0)
Hematocrit (%)	42 ± 5	42 ± 4

Data are presented as mean ± standard deviation

CABG coronary artery bypass grafting, *PCI* percutaneous coronary intervention

370; Bayer Schering Pharma, Berlin, Germany). Prospectively electrocardiography (ECG)-triggered coronary CT angiogram (CTA) was acquired 10 min after the stress perfusion CT with 26 mgI/kg/s of Iopamiron (0.84 mL/kg). The total volume of the injected contrast material before delayed-phase CT was adjusted so that the total volume would reach 600 mgI/kg (1.6 mL/kg) [3]. End-systolic (250 ms after R wave) delayed CT images were acquired at 3, 5 and 7 min after coronary CTA using prospectively ECG-triggered axial scans using cardiac shuttle mode [3] and reconstructed with 1-mm slice thickness with a Qr36d kernel. Tube voltage was 80 kVp while tube current was automatically determined by automatic exposure control system with quality reference mAs set at 580 mAs/80 kVp.

Image post-processing and analysis

Delayed images at 3, 5 and 7 min were reformatted in short axis of left ventricle with slice thickness of 6 mm, average intensity projection and narrow window settings; window width of 150–200 and window level of 100 (Fig. 2a). Qualitative image quality analysis was performed with a score between 1 and 4 (Fig. 3), where 1 means poor image quality with infarct scar barely evident, 2 means moderate image quality causing low diagnostic confidence (loss of clear delineation in all parts), 3 is good image quality (good delineation of infarct scar in most parts) and 4 is excellent image quality (sharply defined borders with good delineation of infarct scar in all parts) [19]. A total of 105 datasets (35 patients × 3 time points) were presented to two independent

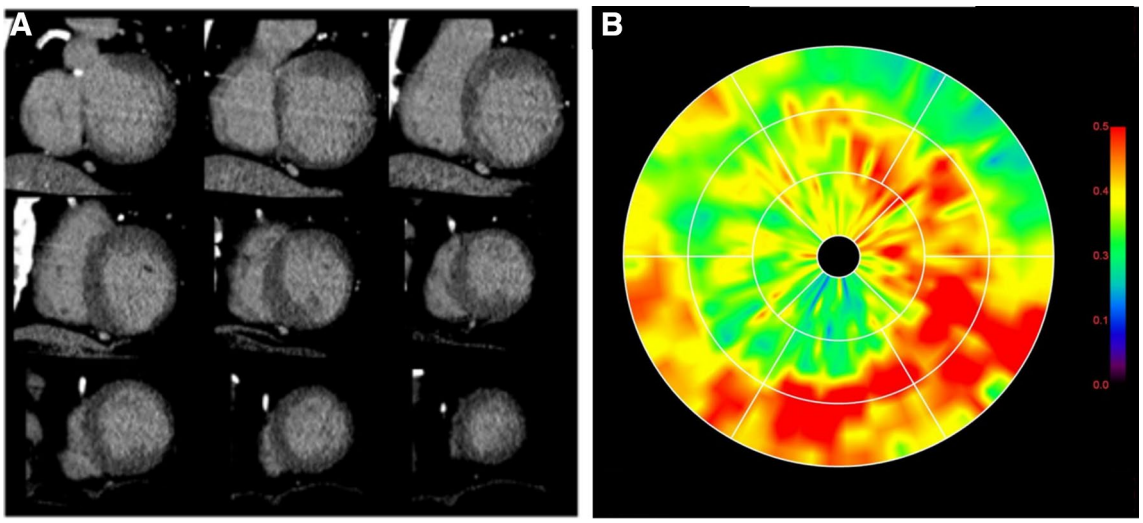

Fig. 2 An example of image analysis in a patient with inferolateral myocardial infarction. Delayed images at 3, 5 and 7 min were reformatted in short axis of left ventricle with slice thickness of 6 mm, average intensity projection and narrow window settings; window width of 150–200 and window level 100 for qualitative image analysis (**a**). Extracellular volume (ECV) was calculated based on a subtraction between delayed images and unenhanced images after non-rigid registration, and final result was shown in a polar map display. Increase of ECV in infarcted myocardium in the inferolateral wall can be appreciated in red color (**b**). Global ECV value as well as mean ECV values for each of 16 American Heart Association myocardial segments were obtained from the polar map

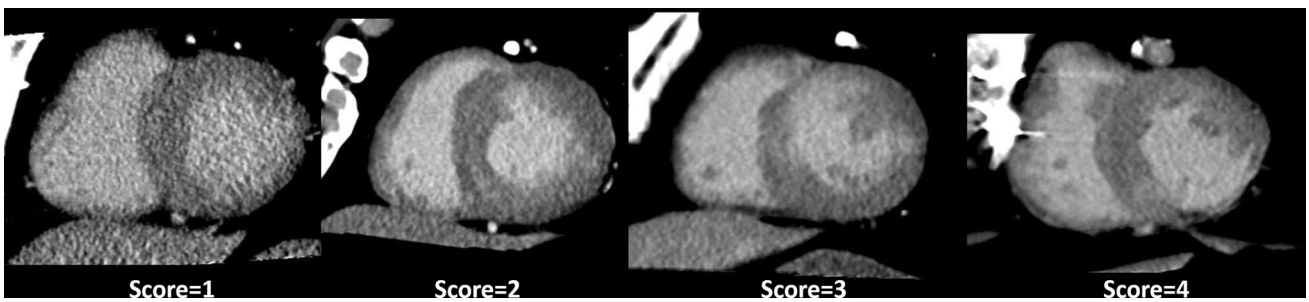

Fig. 3 An example of qualitative image quality analysis where images were assigned scores between 1 and 4. In images with score 1, the infarct scar at the lateral wall of the left ventricle is barely evident. In score 2, loss of clear delineation in all parts of the small scar at the anterior wall is noted. In score 3, good delineation of the anteroseptal wall infarct scar in most parts. In images with score 4, sharply defined borders and good delineation of the inferolateral wall infarct scar is seen in all parts

observers (A.H and Y.G) in a random order for image quality assessment. Observers were allowed to adjust window settings according to their personal preferences to provide the best visualization of scars. The transmural extent of the infarcts was also analyzed in the three time points on the patient level by a consensus of the observers. Transmurality was rated on a 3-point scale (1 = subendocardial only, 2 = infarct extends into mid-wall but is not transmural, 3 = transmural) and agreement among the different time points for estimation of the degree of transmurality was assessed. When multiple infarcts were observed in the same patient, the largest infarct was used for the analysis.

In addition, quantitative image quality analysis was performed by manual drawing of > 0.5 cm^2 regions of interest (ROI) on the infarct scar, remote myocardium, and blood pool. ROIs at the remote myocardium and blood pool were drawn within the same slice containing the ROI at the infarct scar. Areas of fatty infiltration in MI were carefully excluded from the drawn ROI. Attenuation values were tracked at three different slice positions, and the mean value was used for analysis [20]. Signal-to-noise (SNR) ratio which is the mean attenuation of remote myocardium divided by SD of remote myocardial attenuation [3], and contrast-to-noise ratio (CNR) which is defined as the difference in attenuation of scar and remote myocardium divided by the standard deviation (SD) of the remote myocardial attenuation [18] were also quantified.

For ECV calculation, a commercial software (CT myocardial ECV analysis; Ziosoft Inc., Tokyo, Japan) employing the following equation was used: ECV = (ΔHUm/ΔHUb) × (1 − Hct), where ΔHUm is the change in attenuation of the myocardium in Hounsfield unit (HU), ΔHUb is the change in attenuation of the blood pool, and Hct is the hematocrit level. ΔHU = HUdelay − HUpre, where HUdelay and HUpre are attenuation values at delayed-phase and unenhanced CT, respectively [21]. Unenhanced images were subtracted from delayed-phase images using automatic, nonrigid image registration function. Subendocardial and subepicardial borders were contoured automatically. Manual editing of cardiac contours was performed when necessary. The software finally produces a polar map showing 16 American Heart Association myocardial segments with the mean ECV value for each segment as well as the global ECV value (Fig. 2b). In patients showing MI pattern of delayed enhancement, 16 segments were divided into those with delayed enhancement (MI segments) and those without (remote segments). ECV values in MI and remote segments were separately averaged in each patient.

Radiation dose

Values of the dose-length product (DLP) reported by the scanner were recorded for each phase of the study protocol and for the entire study. DLP was kept constant for each of the three time points of the delayed acquisition. Effective radiation doses were estimated by multiplying the DLP by a conversion factor of 0.014 mSv/mGy/cm according to standard methodology outlined in guidelines [22].

Statistical analysis

All values are expressed as mean ± standard deviation (SD). A P-value of < 0.05 indicates statistical significance. Student t test was used to compare continuous variable values between two groups while the Wilcoxon signed rank test was used to compare the median difference of categorical data between two groups. Continuous variables of more than two groups were compared with one-way repeated-measures analysis of variance (ANOVA) with Bonferroni post-hoc test and categorical data were compared with Friedman test and Dunn's post-hoc test. The inter-observer agreement for image quality assessment was measured with Cohen's kappa (k). Agreement among the three time points on the degree of transmural extension was assessed with the Fleiss Kappa test. The statistical analysis was performed using IBM SPSS Statistics 18 (IBM Corporation, Armonk, NY) and GraphPad PRISM 6 (GraphPad Software, Inc, La Jolla, CA).

Results

Image quality and infarct transmurality

Infarct scar of the 35 patients could successfully be identified at all of the three time points without severe artifacts that may mask presence of delayed enhancement. For observer 1, Friedman test showed significant difference ($p = 0.003$) where the 3 min' group had significantly lower image quality (2.5 ± 1.1) while the 5 and 7 min had almost the same image quality scores (2.9 ± 0.9 and 3.0 ± 0.8, respectively). For observer 2, no statistically significant difference was found between the different time points although the highest score was observed at 5 min (2.9 ± 0.9 at 3, 3.1 ± 0.8 at 5 and 2.9 ± 0.95 at 7 min) (Fig. 4). The inter-observer agreement of scoring was good for all time points but was highest at 5 min (Cohen Kappa = 0.61, 0.70 and 0.67 for 3, 5 and 7 min, respectively). An example of image quality at different time point is presented in Fig. 5.

Transmural extent was stable throughout 3, 5, 7 min in 28 (80%) of patients (n = 7, 7 and 14 for grade 1, 2, 3, respectively). Using Kappa statistics, excellent agreement was noted among the three time points for transmurality estimation (Fleiss Kappa = 0.84). The best agreement (33/35, 94.3%) was noted between 5 and 7 min (Cohen Kappa = 0.91) (online supplementary tables).

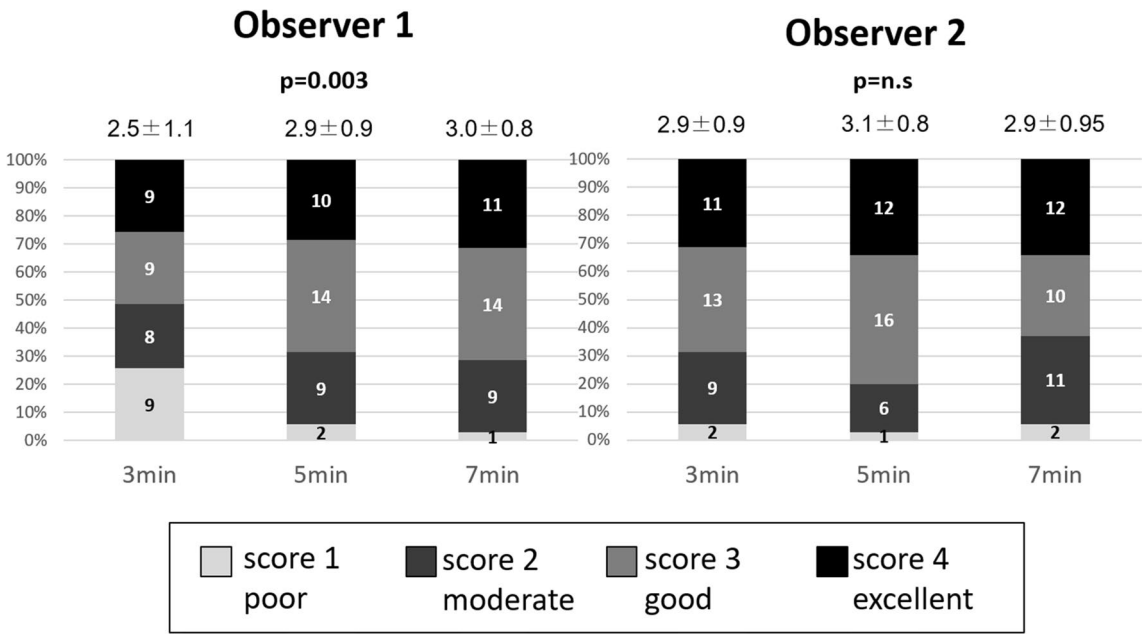

Fig. 4 Image quality scores for both observers. For observer 1, image quality scores at 5 and 7 min were significantly higher than 3 min. For observer 2, highest score was observed at 5 min, however, this difference was not statistically significant

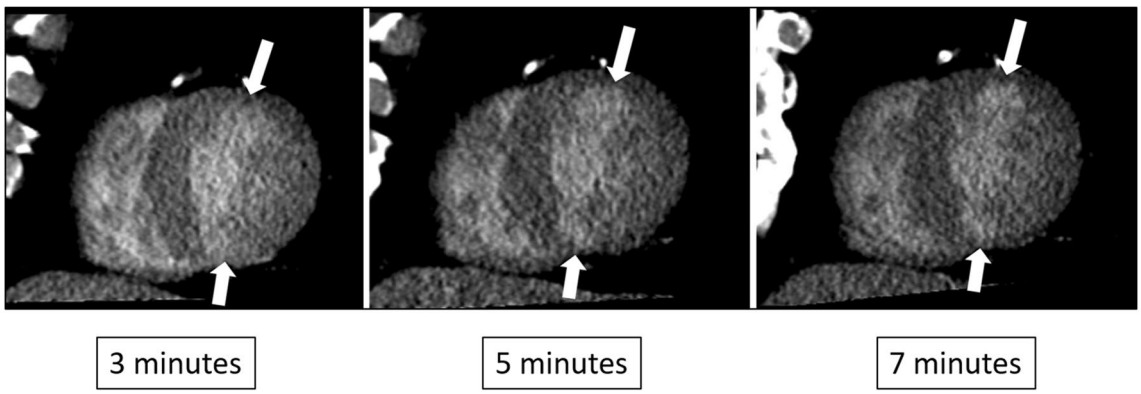

Fig. 5 Delayed enhancement CT at 3 (left), 5 (middle) and 7 (right) minutes after contrast material injection in a 63 years old male with small infarctions in anterior and inferior walls (arrows). The infarcted tissues are barely visible at 3 min but are clearly demonstrated at 5 and 7 min. The image at 7 min has slightly better image quality than at 5 min. The images at 3, 5 and 7 min were given the scores of 1,3,3 and 3,3,3 by observer 1 and observer 2, respectively

SNR and CNR

SNR at 5 min (15.2 ± 1) was slightly but significantly higher than that at 3 and 7 min (13.6 ± 1.0 at 3 min, $p < 0.0001$ and 14.9 ± 1.0 at 7 min, $p = 0.0015$). As for CNR, values at 7 min were about 28% higher than at 3 min (6.4 ± 2.5 at 7 min and 5.0 ± 1.9 at 3 min, $p < 0.0001$), while no significant difference was observed between 5 and 7 min (6.1 ± 2.2 at 5 min, $p = 0.08$) (Fig. 6). HU values of the blood pool, MI site and remote myocardium are presented in Table 2.

ECV

For the normal myocardium in control subjects, no significant difference was found in global ECV values among the three time points (27.6% ± 2.4% vs. 27.1% ± 2.1% vs. 27% ± 2.3% at 3, 5 and 7 min, respectively, $p = 0.26$ by one-way ANOVA repeated measures) (Fig. 7).

Likewise, for the remote myocardial segments in MI patients, ECV values remained nearly unchanged among the three time points (27.7% ± 3.3%, 27.2% ± 3.0% and 27.3% ± 3.2% at 3, 5 and 7 min, respectively, $p = 0.22$). In

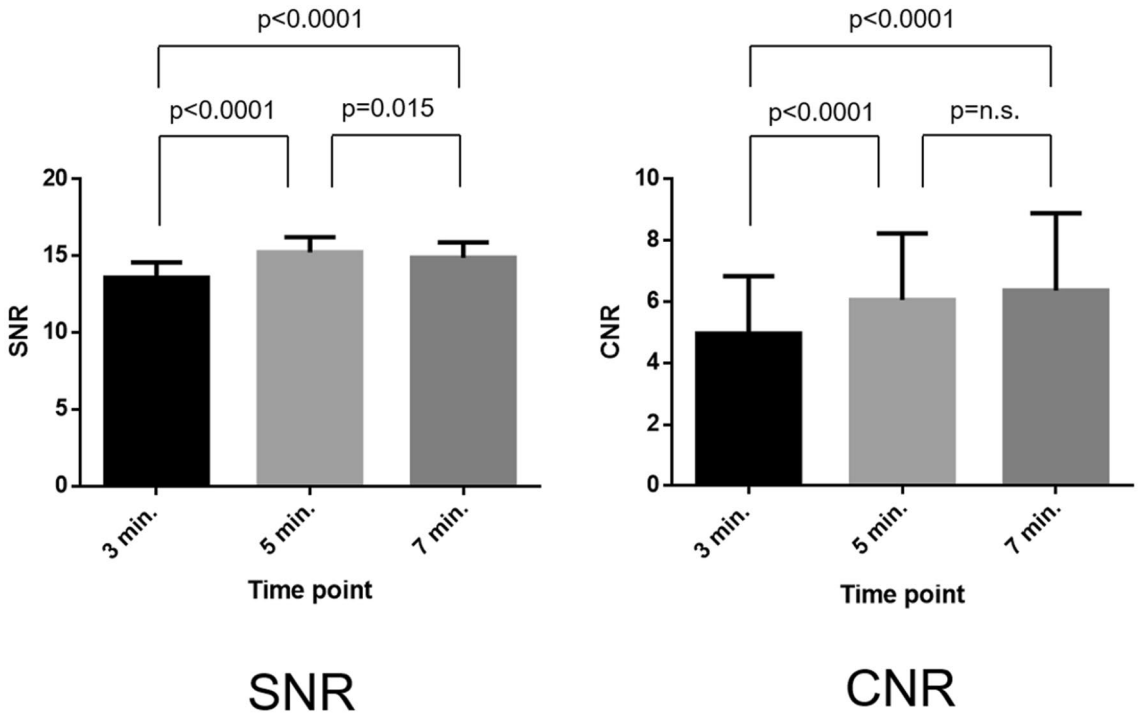

Fig. 6 Bar graph showing SNR (left) and CNR (right) for the 3, 5 and 7 min time points of delayed CT acquisitions. The highest SNR was seen at 5 min. The highest CNR was achieved at 7 min, though was not significantly different from CNR at 5 min

Table 2 HU of left ventricular blood pool, infarct tissue and remote myocardium at 3, 5 and 7 min post-contrast administration

	3 min	5 min	7 min
Left ventricular blood pool	162.4 ± 14.6	144 ± 12.4	134.2 ± 10.7
Infarct tissue	144.8 ± 15.5	134.8 ± 13.8	131 ± 15.6
Remote myocardium	106.4 ± 7.8	96.5 ± 6.3	92 ± 6.2

Data are presented as mean ± standard deviation

MI segments, ECV values showed a trend of lower value at 3 min in comparison with 5 and 7 min (38.7% ± 5% at 3, 39.6% ± 5.3% at 5 and 39.8% ± 5.6% at 7 min, $p = 0.06$).

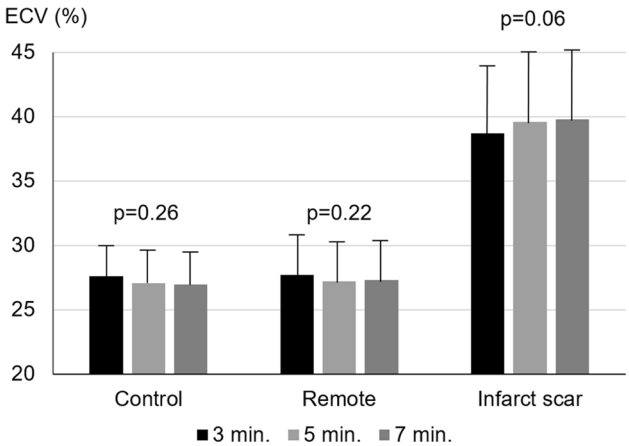

Fig. 7 Bar graph showing ECV fractions at 3, 5 and 7 min at the myocardial infarction (MI), remote myocardium and myocardium in control subjects. In MI segments, 7 min yielded the highest ECV values but was not significantly different from those at 5 min. In infarct-free myocardium, no difference was noticed in ECV estimates among the different time points

Radiation dose

Details of DLP and estimated effective radiation doses are shown in Table 3. The DLP of the delayed phase CT was 211.9 ± 43.8 mGy/cm for the three time points combined, with a calculated effective radiation dose of 2.9 ± 0.61 mSv. For the entire CT examination, DLP was 839.5 ± 201.9 mGy/cm (effective radiation dose of 11.8 ± 2.9 mSv).

Discussion

The results of our study demonstrate that:

1. For visualization of infarct scar with cardiac CT delayed phase imaging, images acquired at 5 and 7 min had significantly higher CNR and image quality than those at 3 min. The 5 min' time point provides equally high image quality and CNR as the later time point at 7 min.

Table 3 Dose length product and estimated effective radiation dose for each phase of the study and for the entire study protocol

Study phase	Dose length product (mGy/cm)	Estimated effective radiation dose (mSv)
Pre-contrast CT	57.6 ± 30.8	0.8 ± 0.43
Dynamic perfusion CT	260.4 ± 73.3	3.6 ± 1.0
Coronary CT angiography	216.4 ± 121.4	3.0 ± 1.7
Delayed enhancement CT (three time points combined)	211.9 ± 43.8	2.9 ± 0.61
Entire study protocol	839.5 ± 201.9	11.8 ± 2.9

Data are presented as mean ± standard deviation

2. Myocardial ECV fraction estimated by CT was stable in the infarct-free myocardium and focal scars among delay time of 3, 5, and 7 min.

Cardiac CT, particularly delayed enhancement CT has a promising potential for more engaging role in viability assessment. Multiple animal and human studies compared cardiac CT to late gadolinium enhancement MRI, which is the current gold standard for viability assessment, and showed good agreement between both modalities for the detection and the estimation of the infarct size [11, 13, 15, 17]. Good agreement and significant correlation was also found for the CT and MRI-derived ECV fractions [21, 23–25]. Radiation exposure in CT has always been a concern. However, with new CT technologies and using strategies like high pitch mode and prospective ECG triggering, delayed enhancement CT can be performed with lower than 1 mSv radiation dose [26]. Despite the fact that CNR of MRI is considerably higher than that of CT, CT is advantageous in terms of the fast scanning times, the excellent spatial resolution and its suitability for patients with implanted electronic devices such as cardiac pacemakers. In addition, with the use of new reconstruction algorithms, improved CNR and less artifacts can be achieved [3].

Till this moment, no consensus is yet available on the perfect timing for delayed image acquisition. Human studies on delayed phase cardiac CT used different time points that range from 5 to 15 min post contrast administration [3, 10–18]. In our study, despite myocardial scars could be successfully identified at 3 min with excellent agreement on the degree of transmural extent with the rest of the time points, its image quality scores and CNR were significantly lower compared to 5 and 7 min' time points. The highest CNR between the infarcted and normal myocardium was achieved at 7 min, however, the values were very similar to those at 5 min with no statistically significant difference. Image quality scores were comparable at 5 and 7 min.

Similar results have been reported in an animal study using porcine models of acute and subacute infarcts. Brodoefel et al. compared images acquired at 3, 5, 10 and 15 min' time points for both the bolus and the bolus/low flow injection protocols and reported that the best image quality was achieved at 5 min with the bolus injection protocol and at 5 and 10 min with the bolus/low flow protocol [20, 27]. Although our assessments focused on visualization of chronic infarct scar with bolus injection protocol, we agree that the earlier 3 min' time point is of significantly lower image quality than later time points.

Our results are also in line with Jacquier et al. who compared 5 and 10 min' time points in 19 reperfused acute MI patients and reported that image quality and SNR were significantly higher at 5 min compared to 10 min post contrast administration [9]. Instead of the 10 min, we used an earlier time point of 7 min which explains the similar results with 5 min and suggests that time points later than 7 min are likely to be of lower image quality.

Another aim of our study was to assess the impact of acquisition timing on ECV fraction estimation in myocardium with and without focal scar. For the myocardium without scar tissue, estimated ECV fraction was stable for 3, 5, 7 min time points for both control subjects and remote myocardium of MI patients. Our results are in line with a recent CT study by Jablonowski et al. which demonstrated that in control animals, an equilibrium state could be achieved within the first minute after contrast administration and that ECV values remained almost the same in all time points [28]. ECV values in normal myocardium were about 27% which is fairly consistent with previous work and MRI data [21, 29] taking into consideration that this is not a completely normal myocardium, the relatively old age of the study population [14] and the possibility of minor ECV increase due to adenosine-induced vasodilatation since our protocol included stress CT perfusion [30].

There is a very limited number of publications on ECV estimation in chronic MI scars [31], likely because ECV is not of clinical importance for the detection of MI. However, unlike other fibrosis-inducing pathologies which are seldom referred for comprehensive cardiac CT, focal scar of MI is frequently encountered in the routine cardiac CT practice which makes it a suitable candidate for ECV testing. In CMR studies, delayed enhanced images for ECV estimation are usually acquired about 15 min after contrast material administration. This is problematic in cardiac CT because such long periods result in lower CNR due to contrast clearance. Jerosch-Herold et al. performed simulations using a model of blood-to-tissue exchange of contrast agent to test the equilibrium assumption for a bolus injection protocol. They reported that, apart from tissues with extremely low perfusion (less than 0.1 ml/min/g), a state of equilibrium could be reached at time points starting from 3 min after

contrast agent injection [32]. In fact, ECV in the infarct scars were stable among 3, 5, and 7 min without significant difference. To our knowledge, only one recent cardiac CT study by Treibel at al. reported the effect of acquisition timing on the measured ECV values [24]. They compared the ECV fraction in amyloidosis patients measured from 5 and 10 min acquisitions after contrast bolus injection and found that the 5 min' ECV fraction was better correlated with MRI-derived ECV. Our findings suggest that dynamic equilibrium can even be achieved as early as 3 min post contrast administration.

The stability of ECV measurements in the infarct-free myocardium is ought to the fast exchange of the contrast media between intravascular and extravascular compartments achieving an early state of dynamic equilibrium. This is well documented in cardiac MRI studies as well [33, 34]. In the infarct tissue, despite the expected suboptimal wash-in, wash-out kinetics, ECV measurements were also stable as early as 3 min after CTA. This might be explained by the relatively large amounts of contrast material needed for CTA compared to those used in LGE-MRI which can accelerate the state of equilibrium. In addition, the use of 40 mL of contrast medium in the early perfusion CT phase may have allowed for a partial state of equilibrium before the main dose of the contrast medium was injected in the CTA study.

The comprehensive nature of our cardiac CT protocol as well as the acquisition of delayed enhancement images at three time points led to a total effective radiation dose of 11.8 ± 2.9 mSv. However, all phases of the comprehensive protocol were clinically justified and requested by the referring physicians in our institute. Beside the accumulating evidence of the high diagnostic accuracy of dynamic perfusion CT [35], the acquisition of delayed enhancement images led to the detection of silent myocardial infarction in about 40% of patients referred for comprehensive protocol and subsequent coronary angiography [36]. Our CT late enhancement protocol is based on method proposed by Kurobe et al. [3]. In their approach, four image stacks are acquired during one breath-holding after 7 min of CTA, and then, the four image stacks are averaged after non-rigid registration for noise reduction. In the current study, instead of obtaining four image stacks at 7 min, only one stack was obtained at each of 3, 5 and 7 min. Accordingly, we achieved a radiation dose of 2.9 ± 0.61 mSv for the three delayed acquisitions combined which is still comparable with the dose required for delayed-enhancement CT in previous literature (mean dose, 0.9–4.5 mSv) [12, 13, 17, 18, 26, 37, 38].

Our study had several limitations. First, the study population was small, consisted solely of patients with chronic infarct scar and did not include acute ischemic injury or other non-ischemic diseases causing myocardial fibrosis like cardiomyopathies or amyloidosis. Second, time points later than 7 min were not tested in our study. However, our aim was to identify the earliest possible time point for confident diagnosis of scar tissues. Also, we wanted to avoid excessive radiation exposure to the study participants. We also used only the bolus technique for contrast material injection and did not test the slow infusion technique. However, our aim was to test the technique used by most centers in clinical practice to determine the equilibrium time point. Finally, correlation with cardiac MRI, particularly MRI-derived ECV was not performed in our study as the main purpose was to determine the equilibrium point in CT before making such correlation.

Conclusion

Myocardial scars are equally best visualized with delay time of 5 and 7 min post contrast administration. No significant difference was observed in ECV of healthy myocardium or focal scars among delay time of 3, 5, and 7 min. Delay time of 5 min after contrast injection may be recommended for CT delayed enhancement imaging.

Compliance with ethical standards

Conflict of interest One of the authors (H.S.) received a research grant from DAIICHI SANKYO COMPANY, LIMITED, Fuji Pharma Co., Ltd., FUJIFILM RI Pharma Co., Ltd., Eisai Co., Ltd. All the other authors have nothing to disclose.

References

1. Aikawa T, Oyama-Manabe N, Naya M, Ohira H, Sugimoto A, Tsujino I, Obara M, Manabe O, Kudo K, Tsutsui H, Tamaki N (2017) Delayed contrast-enhanced computed tomography in patients with known or suspected cardiac sarcoidosis: a feasibility study. Eur Radiol 27:4054–4063
2. Tanabe Y, Kido T, Kurata A, Kouchi T, Fukuyama N, Yokoi T, Uetani T, Yamashita N, Miyagawa M, Mochizuki T (2018) Late iodine enhancement computed tomography with image subtraction for assessment of myocardial infarction. Eur Radiol 28:1285–1292
3. Kurobe Y, Kitagawa K, Ito T, Kurita Y, Shiraishi Y, Nakamori S, Nakajima H, Nagata M, Ishida M, Dohi K (2014) Myocardial delayed enhancement with dual-source CT: advantages of targeted spatial frequency filtration and image averaging over half-scan reconstruction. J Cardiovasc Comput Tomogr 8:289–298
4. Omori T, Kurita T, Dohi K, Takasaki A, Nakata T, Nakamori S, Fujimoto N, Kitagawa K, Hoshino K, Tanigawa T, Sakuma H, Ito M (2018) Prognostic impact of unrecognized myocardial scar in the non-culprit territories by cardiac magnetic resonance imaging in patients with acute myocardial infarction. Eur Heart J Cardiovasc Imaging 19:108–116
5. Becker MAJ, Cornel JH, van de Ven PM, van Rossum AC, Allaart CP, Germans T (2018) The prognostic value of late gadolinium-enhanced cardiac magnetic resonance imaging in nonischemic dilated cardiomyopathy: a review and meta-analysis. JACC Cardiovasc Imaging 11:1274–1284

6. Hulten E, Agarwal V, Cahill M, Cole G, Vita T, Parrish S, Bittencourt MS, Murthy VL, Kwong R, Di Carli MF (2016) Presence of late gadolinium enhancement by cardiac magnetic resonance among patients with suspected cardiac sarcoidosis is associated with adverse cardiovascular prognosis clinical perspective: a systematic review and meta-analysis. Circ Cardiovasc Imaging 9:e005001
7. Zhuang B, Sirajuddin A, Wang S, Arai A, Zhao S, Lu M (2018) Prognostic value of T1 mapping and extracellular volume fraction in cardiovascular disease: a systematic review and meta-analysis. Heart Fail Rev 23:723–731
8. Mendoza DD, Joshi SB, Weissman G, Taylor AJ, Weigold WG (2010) Viability imaging by cardiac computed tomography. J Cardiovasc Comput Tomogr 4:83–91
9. Jacquier A, Boussel L, Amabile N, Bartoli JM, Douek P, Moulin G, Paganelli F, Saeed M, Revel D, Croisille P (2008) Multidetector computed tomography in reperfused acute myocardial infarction: assessment of infarct size and no-reflow in comparison with cardiac magnetic resonance imaging. Investig Radiol 43:773–781
10. Boussel L, Ribagnac M, Bonnefoy E, Staat P, Elicker BM, Revel D, Douek P (2008) Assessment of acute myocardial infarction using MDCT after percutaneous coronary intervention: comparison with MRI. Am J Roentgenol 191:441–447
11. Choe YH, Choo KS, Jeon E-S, Gwon H-C, Choi J-H, Park J-E (2008) Comparison of MDCT and MRI in the detection and sizing of acute and chronic myocardial infarcts. Eur J Radiol 66:292–299
12. George RT, Arbab-Zadeh A, Miller JM, Vavere AL, Bengel FM, Lardo AC, Lima JA (2012) Computed tomography myocardial perfusion imaging with 320-row detector computed tomography accurately detects myocardial ischemia in patients with obstructive coronary artery disease. Circ Cardiovasc Imaging 5:333–340
13. Gerber BL, Belge B, Legros GJ, Lim P, Poncelet A, Pasquet A, Gisellu G, Coche E, Vanoverschelde J-LJ (2006) Characterization of acute and chronic myocardial infarcts by multidetector computed tomography comparison with contrast-enhanced magnetic resonance. Circulation 113:823–833
14. Kurita Y, Kitagawa K, Kurobe Y, Nakamori S, Nakajima H, Dohi K, Ito M, Sakuma H (2016) Estimation of myocardial extracellular volume fraction with cardiac CT in subjects without clinical coronary artery disease: a feasibility study. J Cardiovasc Comput Tomogr 10:237–241
15. Lardo AC, Cordeiro MA, Silva C, Amado LC, George RT, Saliaris AP, Schuleri KH, Fernandes VR, Zviman M, Nazarian S (2006) Contrast-enhanced multidetector computed tomography viability imaging after myocardial infarction characterization of myocyte death, microvascular obstruction, and chronic scar. Circulation 113:394–404
16. Lessick J, Dragu R, Mutlak D, Rispler S, Beyar R, Litmanovich D, Engel A, Agmon Y, Kapeliovich M, Hammerman H (2007) Is functional improvement after myocardial infarction predicted with myocardial enhancement patterns at multidetector CT? 1. Radiology 244:736–744
17. Mahnken AH, Koos R, Katoh M, Wildberger JE, Spuentrup E, Buecker A, Günther RW, Kühl HP (2005) Assessment of myocardial viability in reperfused acute myocardial infarction using 16-slice computed tomography in comparison to magnetic resonance imaging. J Am Coll Cardiol 45:2042–2047
18. Nieman K, Shapiro MD, Ferencik M, Nomura CH, Abbara S, Hoffmann U, Gold HK, Jang I-K, Brady TJ, Cury RC (2008) Reperfused myocardial infarction: contrast-enhanced 64-section CT in comparison to MR imaging 1. Radiology 247:49–56
19. Brodoefel H, Klumpp B, Reimann A, Ohmer M, Fenchel M, Schroeder S, Miller S, Claussen C, Kopp A, Scheule A (2007) Late myocardial enhancement assessed by 64-MSCT in reperfused porcine myocardial infarction: diagnostic accuracy of low-dose CT protocols in comparison with magnetic resonance imaging. Eur Radiol 17:475–483
20. Brodoefel H, Reimann A, Klumpp B, Fenchel M, Ohmer M, Miller S, Schroeder S, Claussen C, Scheule A, Kopp AF (2007) Assessment of myocardial viability in a reperfused porcine model: evaluation of different MSCT contrast protocols in acute and subacute infarct stages in comparison with MRI. J Comput Assisted Tomogr 31:290–298
21. Nacif MS, Kawel N, Lee JJ, Chen X, Yao J, Zavodni A, Sibley CT, Lima JA, Liu S, Bluemke DA (2012) Interstitial myocardial fibrosis assessed as extracellular volume fraction with low-radiation-dose cardiac CT. Radiology 264:876–883
22. Halliburton SS, Abbara S, Chen MY, Gentry R, Mahesh M, Raff GL, Shaw LJ, Hausleiter J (2011) SCCT guidelines on radiation dose and dose-optimization strategies in cardiovascular CT. J Cardiovasc Comput Tomogr 5:198–224
23. Kurita Y, Kitagawa K, Kurobe Y, Nakamori S, Nakajima H, Dohi K, Ito M, Sakuma H (2016) Data on correlation between CT-derived and MRI-derived myocardial extracellular volume. Data Brief 7:1045–1047
24. Treibel TA, Bandula S, Fontana M, White SK, Gilbertson JA, Herrey AS, Gillmore JD, Punwani S, Hawkins PN, Taylor SA (2015) Extracellular volume quantification by dynamic equilibrium cardiac computed tomography in cardiac amyloidosis. J Cardiovasc Comput Tomogr 9:585–592
25. Bandula S, White SK, Flett AS, Lawrence D, Pugliese F, Ashworth MT, Punwani S, Taylor SA, Moon JC (2013) Measurement of myocardial extracellular volume fraction by using equilibrium contrast-enhanced CT: validation against histologic findings. Radiology 269:396–403
26. Goetti R, Feuchtner G, Stolzmann P, Donati OF, Wieser M, Plass A, Frauenfelder T, Leschka S, Alkadhi H (2011) Delayed enhancement imaging of myocardial viability: low-dose high-pitch CT versus MRI. Eur Radiol 21:2091
27. Brodoefel H, Klumpp B, Reimann A, Fenchel M, Heuschmid M, Miller S, Schroeder S, Claussen C, Scheule A, Kopp A (2007) Sixty-four-MSCT in the characterization of porcine acute and subacute myocardial infarction: determination of transmurality in comparison to magnetic resonance imaging and histopathology. Eur J Radiol 62:235–246
28. Jablonowski R, Wilson MW, Do L, Hetts SW, Saeed M (2014) Multidetector CT measurement of myocardial extracellular volume in acute patchy and contiguous infarction: validation with microscopic measurement. Radiology 274:370–378
29. Puntmann VO, Voigt T, Chen Z, Mayr M, Karim R, Rhode K, Pastor A, Carr-White G, Razavi R, Schaeffter T (2013) Native T1 mapping in differentiation of normal myocardium from diffuse disease in hypertrophic and dilated cardiomyopathy. JACC: Cardiovasc Imaging 6:475–484
30. Mahmod M, Piechnik SK, Levelt E, Ferreira VM, Francis JM, Lewis A, Pal N, Dass S, Ashrafian H, Neubauer S (2014) Adenosine stress native T1 mapping in severe aortic stenosis: evidence for a role of the intravascular compartment on myocardial T1 values. J Cardiovasc Magn Reson 16:92
31. Sado DM, Flett AS, Banypersad SM, White SK, Maestrini V, Quarta G, Lachmann RH, Murphy E, Mehta A, Hughes DA (2012) Cardiovascular magnetic resonance measurement of myocardial extracellular volume in health and disease. Heart 98:1436–1441
32. Jerosch-Herold M, Sheridan DC, Kushner JD, Nauman D, Burgess D, Dutton D, Alharethi R, Li D, Hershberger RE (2008) Cardiac magnetic resonance imaging of myocardial contrast uptake and blood flow in patients affected with idiopathic or familial dilated cardiomyopathy. Am J Physiol Heart Circ Physiol 295:H1234–H1242
33. Klein C, Nekolla SG, Balbach T, Schnackenburg B, Nagel E, Fleck E, Schwaiger M (2004) The influence of myocardial blood

flow and volume of distribution on late Gd-DTPA kinetics in ischemic heart failure. J Magn Reson Imaging 20:588–594
34. Ugander M, Oki AJ, Hsu L-Y, Kellman P, Greiser A, Aletras AH, Sibley CT, Chen MY, Bandettini WP, Arai AE (2012) Extracellular volume imaging by magnetic resonance imaging provides insights into overt and sub-clinical myocardial pathology. Eur Heart J 33:1268–1278
35. Kitagawa K, Goto Y, Nakamura S, Takafuji M, Hamdy A, Ishida M, Sakuma H (2018) Dynamic CT perfusion imaging: state of the art. Cardiovasc Imaging Asia 2:38–48
36. Goto Y, Kitagawa K, Uno M, Nakamori S, Ito T, Nagasawa N, Dohi K, Sakuma H (2017) Diagnostic accuracy of endocardial-to-epicardial myocardial blood flow ratio for the detection of significant coronary artery disease with dynamic myocardial perfusion dual-source computed tomography. Circ J 81:1477–1483
37. Blankstein R, Shturman LD, Rogers IS, Rocha-Filho JA, Okada DR, Sarwar A, Soni AV, Bezerra H, Ghoshhajra BB, Petranovic M, Loureiro R, Feuchtner G, Gewirtz H, Hoffmann U, Mamuya WS, Brady TJ, Cury RC (2009) Adenosine-induced stress myocardial perfusion imaging using dual-source cardiac computed tomography. J Am Coll Cardiol 54:1072–1084
38. Reimann AJ, Kuettner A, Klumpp B, Heuschmid M, Schumacher F, Teufel M, Beck T, Burgstahler C, Schröder S, Claussen CD (2008) Late enhancement using multidetector row computer tomography: a feasibility study with low dose 80 kV protocol. Eur J Radiol 66:127–133